MOLECULAR AND CELLULAR BIOLOGY, Nov. 2001, p. 8189–8196 Vol. 21, No. 23
0270-7306/01/$04.00+0 DOI: 10.1128/MCB.21.23.8189–8196.2001

Regulatory Mechanisms at the Mouse *Igf2*/*H19* Locus

CHRISTOPHER R. KAFFER, ALEX GRINBERG, AND KARL PFEIFER*

Laboratory of Mammalian Genes and Development, National Institute of Child Health and Human Development, Bethesda, Maryland 20892

Received 23 May 2001/Returned for modification 19 July 2001/Accepted 28 August 2001

The closely linked *H19* and *Igf2* genes show highly similar patterns of gene expression but are reciprocally imprinted. *H19* is expressed almost exclusively from the maternally inherited chromosome, while *Igf2* expression is mostly from the paternal chromosome. In humans, loss of imprinting at this locus is associated with tumors and with developmental disorders. Monoallelic expression at the imprinted *Igf2*/*H19* locus occurs by at least two distinct mechanisms: a developmentally regulated silencing of the paternal *H19* promoter, and transcriptional insulation of the maternal *Igf2* promoters. Both mechanisms of allele-specific silencing are ultimately dependent on a common *cis*-acting element located just upstream of the *H19* promoter. The coordinated expression patterns and some experimental data support the idea that positive regulatory elements are also shared by the two genes. To clarify the organization and function of positive and negative regulatory elements at the *H19*/*Igf2* locus, we analyzed two mouse mutations. First, we generated a deletion allele to localize enhancers used in vivo for expression of both *H19* and *Igf2* in mesodermal tissues to sequences downstream of the *H19* gene. Coincidentally, we demonstrated that some expression of *Igf2* is independent of the shared enhancer element. Second, we used this new information to further characterize an ectopic *H19* differentially regulated region and the associated insulator. We demonstrated that its activity is parent-of-origin dependent. In contrast to recent results from *Drosophila* model systems; we showed that this duplication of a mammalian insulator does not interfere with its normal function. Implications of these findings for current models for monoallelic gene expression at this locus are discussed.

Igf2 and *H19* are closely linked and reciprocally imprinted genes located on the distal end of mouse chromosome 7 (48) (Fig. 1a). The regulation of the two genes has been intensively studied both as a model system for understanding mechanisms of genomic imprinting and because dysregulation of *IGF2* in humans is associated with the developmental disorder Beckwith-Wiedemann syndrome and with many types of tumors (33). The two genes are part of a large cluster of imprinted genes whose organization and monoallelic expression patterns are well conserved between mice and humans (30, 31). *H19* represents one limit of this imprinted cluster, as the next known genes, *Nctc1* and *L23mrp*, are both biallelically expressed (19, 49).

Both *H19* and *Igf2* are highly expressed during fetal and early postnatal development and show essentially identical spatial and temporal specificities. In fact, as suggested by their close linkage, their reciprocal imprinting, and their overlapping expression patterns, the two genes share transcriptional regulatory elements. The paternal silencing of *H19* and maternal repression of *Igf2* both depend on a common *cis*-acting element, here called the *H19ICE* (for *H19* imprinting control element), located upstream of the *H19* promoter (Fig. 1a) (20, 42). The boundaries of the *ICE* are not entirely precise, as they differ depending on the specific assay used. Sequences to kb −7 (relative to the start site of the *H19* mRNA transcript) are sufficient to imprint single-copy *H19* transgenes (20). If sequences to only kb −3.8 are used, only transgenes inserted as multiple copies are imprinted, and even then paternally inherited *H19* transgenes are expressed in occasional pups (32). Deletion of endogenous sequences between kb −3.8 and 2.0 (or between kb −7 and −0.8) on the maternal chromosome results in the loss of imprinting of the paternal *H19* allele. Significantly, the same deletion inherited through the maternal germline results in activation of the normally silent maternal *Igf2* allele (36, 42). The *ICE* includes DNA sequence domains, centered at kb −2.4 and −3.8, that show nuclease hypersensitivity specifically on the maternal chromosome (16, 23, 39). These regions of hypersensitivity were identified in somatic tissue and lie within a 2-kb domain of DNA showing hypermethylation specific to the paternal chromosome (4, 8, 14, 29, 43, 44). This differentially methylated region (*H19DMR*) is hypermethylated on the paternal chromosome at all stages of development and has been demonstrated to have both silencing and insulating activities (7, 9, 17, 20, 21). On the unmethylated maternal chromosome, the *H19ICE* functions as a transcriptional insulator and blocks activation of the *Igf2* promoters by distal enhancer elements. On the paternal chromosome, the methylation imprint at the *H19DMR* acts to disrupt insulator function and thereby allows expression of *Igf2* on that chromosome. Several labs have recently demonstrated that CTCF, a known enhancer-blocking protein, selectively binds to nonmethylated CpG-containing sequences within the *H19DMR*, thus providing a molecular basis for parent-of-origin-specific activity of the insulator (7, 17, 22, 38). Other studies, however, indicate that this model does not explain all aspects of *Igf2* monoallelism and that elements in addition to the *H19DMR* are required for imprinting of *Igf2* (1, 12).

The insulator model for *Igf2* monoallelic expression demands that all *H19* and *Igf2* enhancers be located downstream of the *H19DMR* or its associated insulator, while the coexpres-

* Corresponding author. Mailing address: 9000 Rockville Pike, Building 6B, Room 2B206, NICHD, Bethesda, MD 20892. Phone: (301) 402-0676. Fax: (301) 402-0543. E-mail: kpfeifer@helix.nih.gov.

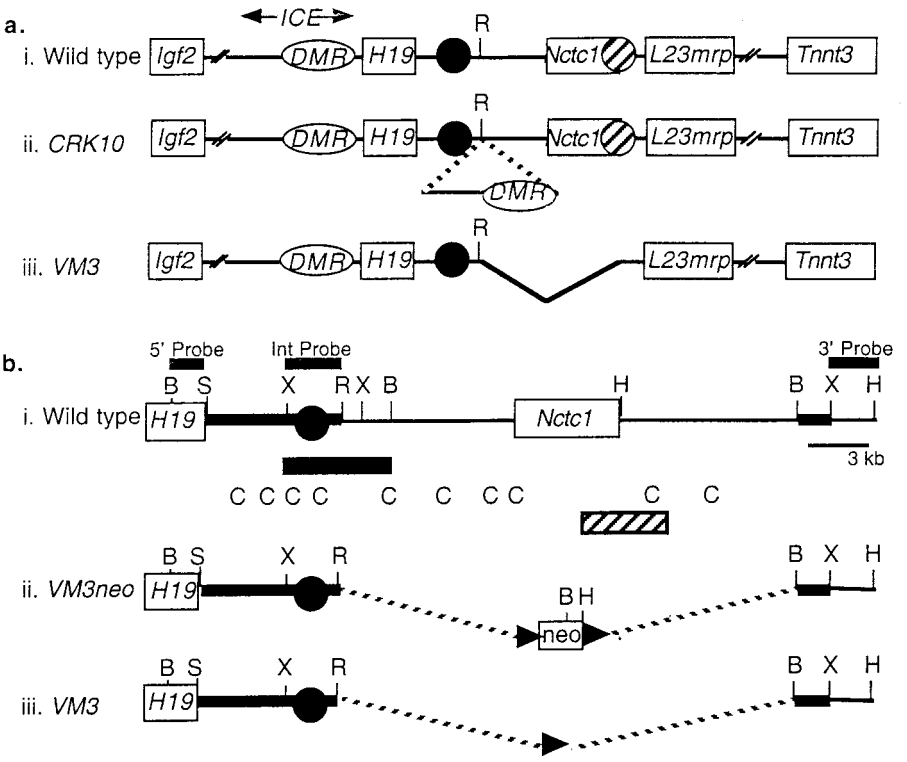

FIG. 1. Diagram of the wild-type, *CRK10*, and *VM3* chromosomes in the *Igf2/H19* region. (a) Summary of the wild-type (i), *CRK10* (ii), and *VM3* (iii) alleles, depicting the relative organization of the *Igf2, H19, Nctc1, L23mrp*, and *Tnnt3* genes (open rectangles). Endodermal and skeletal-muscle-specific enhancers for *H19* and *Igf2* expression are represented by closed and hatched circles, respectively. The mapped locations of these enhancers are based on in vivo analyses of chromosomal deletions (reference 26 and this study) and also on in vitro transfection experiments (20, 46). The *ICE*, for imprinting control element, is defined genetically as the minimal upstream sequence required to imprint single-copy *H19* transgenes (20) and as a sequence whose deletion results in the loss of imprinting of *H19* and *Igf2* (20, 36, 42). Within the *ICE* is the 2-kb *DMR* (for differentially methylated region) (oval) that is hypermethylated specifically on the paternal chromosome (4, 8, 14, 29, 43, 44). Mapping to the *DMR* are domains of maternal-chromosome-specific nuclease hypersensitivity. The *CRK10* allele (ii) carries a 9.2-kb insertion at kb +10.7 (relative to the *H19* transcriptional start site). The inserted DNA includes the *H19DMR*, all the maternal-chromosome-specific nuclease-hypersensitive domains, and additional 5′ sequences that encompass all of the 5′ sequence elements required to imprint single-copy *H19* transgenes (20). The inserted element is the minimal DNA sequence that is known to carry a parent-of-origin-specific transcriptional insulator (reference 20 and this study). The *VM3* allele (iii) deletes sequences showing muscle-specific enhancer activity in vitro and in transgenic mice (18, 20). This deletion encompasses the *Nctc1* gene body. (b) Strategy for construction of the *VM3* allele by deleting from kb +10.7 to +34.7 downstream of the *H19* gene. The wild-type chromosome (i), the targeted *VM3neo* chromosome (ii), and the targeted *VM3* chromosome after Cre recombinase-mediated excision of the neomycin-selectable marker (iii) are depicted. The endodermal enhancers, as defined by in vitro transfection studies, are represented by a closed circle (46). The deletion confirming the role of these enhancers for in vivo expression of both *H19* and *Igf2* is indicated by the closed rectangle below line i (26). Also depicted below line i are sequences conserved between human and mouse (C) (18) as well as sequences showing enhancer activity specifically in myoblast cell lines (hatched rectangle) (20). The flanking sequences used to direct homologous recombination are represented by the thickened lines. Probes used to detect the correctly targeted clones are depicted above line i. B, *Bam*HI; S, *Sal*I; R, *Eco*RI; H, *Hin*dIII; X, *Xba*I.

sion of *Igf2* and *H19* suggests that these enhancer elements are shared. In fact, much of the endoderm-specific expression of both genes is dependent on shared enhancers that must lie between 7.2 and 13 kb downstream of the *H19* promoter and about 80 kb downstream of the *Igf2* promoter (26). However, the location of regulatory elements required to drive expression in mesodermal tissues is less clear. Transgenic mouse and in vitro transfection studies together indicate that enhancers capable of directing expression of *H19* in skeletal muscle are located at between kb +25 and +28 (18, 20). Transgenic studies also suggest that additional enhancer elements that can direct *H19* expression in several tissues, including cardiac muscle, may lie downstream of kb +35 (2, 20). However, neither the necessity of these elements for expression of the *H19* gene in its normal chromosomal location nor their role in the expression of *Igf2* has yet been tested.

In addition to its role in regulating activity of the insulator element, the paternal imprint at the *H19DMR* has a second, genetically distinct function of blocking transcription of the paternal *H19* allele by directing CpG methylation of the paternal *H19* promoter and gene body sequences. Once established, this promoter methylation and associated epigenetic changes are capable of silencing the *H19* promoter independently of the *H19DMR* (36). We have previously generated a mutant allele, *CRK10*, in which the sequences from kb −10 to −0.8 that encompass the *H19DMR* were inserted at the kb +10.7 position (Fig. 1b) (20). As predicted by the insulator model, transcription of *H19* in skeletal muscle was blocked

while expression in liver was unaffected. We also demonstrated that CpGs in the inserted *DMR* element were methylated only when paternally inherited. However, it could not be determined whether this methylation was capable of blocking insulator activity or whether the hypermethylation from the exogenous *H19DMR* could spread to neighboring sequences.

In this study, we generated a 24-kb chromosomal deletion of sequences that included the presumptive mesodermal enhancers, and we further analyzed the *CRK10* insertion mutation to clarify the organization and function of regulatory elements at the *Igf2*/*H19* locus. First, by deletion of the putative mesodermal enhancer elements, we demonstrated that normal expression of *H19* and *Igf2* in both the tongue and limb muscle is dependent on these sequences. However, expression in mesodermal cells in other organs is dependent on additional enhancers downstream of kb +36. We demonstrated the latter point by using the *CRK10* allele of chromosome 7 in which the *H19ICE* has been moved to kb +10.7. In a second set of experiments, we further analyzed the function of this exogenously located *ICE*/*H19DMR*/*Igf2*-insulator. We showed that while the insulator function remained parent-of-origin dependent, in its new location it could not direct methylation of neighboring sequences as it does the *H19* promoter. We also demonstrated that insertion of this second *H19DMR* element had no effect on expression of *Igf2* from the maternal chromosome. Thus, the insertion of a second active insulator element did not interfere with silencing of the maternal *Igf2* gene. Implications of this finding for possible mechanisms of transcriptional insulation are discussed. Finally and parenthetically, we demonstrated that the mouse *Nctc1* gene is not required for normal mouse development or fertility.

MATERIALS AND METHODS

Generation of VM3 mutant mice. For the structure of the flanking sequences used to direct homologous recombination, see Fig. 1b. The targeting vector was linearized and transfected into RI mouse embryonic stem cells. To identify *VM3neo* clones, DNAs from G418-resistant colonies were digested with *Bam*HI and probed with a 1.2-kb *Bam*HI-*Sal*I fragment from just outside the 5′ flank to identify a 11.3-kb band in wild-type cells and an additional 10-kb band in targeted lines. Likewise, digestion with *Hin*dIII and probing with a 4-kb *Hin*dIII-*Xba*I fragment from just outside the 3′ flank identified a 15-kb band in wild-type cells and an additional 5.5-kb band in correctly targeted clones. Two independently derived lines were injected into C57/BL6-J blastocysts to generate chimeric founders. Founder males were mated with mice carrying the *EIIa-cre* transgene (25) to excise neomycin resistance-encoding sequences. Successful excision of the neomycin resistance gene was assayed by digestion with *Xba*I and hybridization to a 2.0-kb internal *Xba*I-*Eco*RI fragment which displays 3.1-, 2.4-, and 4.3-kb bands for the *VM3*, wild-type, and *VM3neo* alleles, respectively.

RNA analysis. Tissues were homogenized in TRIZOL reagent (Life Technologies) by using a power homogenizer, and the RNA was isolated according to the manufacturer's protocol. Expression levels were analyzed by Northern blotting. Probes used to quantitate *H19, Igf2*, and EF2a RNAs were described previously (20). cDNA from p6 skeletal muscle was amplified using *L23mrp*-specific primers (5′-ATGTGTTGTACCCCCTTTACC-3′ and 5′-TGGTCCAAATCCTGCTGTC-3′) to obtain a 455-bp probe or using *Tnnt3*-specific primers (5′-AGAAGAGAGGAGGAGGATG-3′ and 5′-GTGCAGAGCTGGAATAAG-3′) to obtain a 475-bp probe. Expression levels were quantified with the Molecular Dynamics Storm PhosphorImaging System.

Allele-specific expression of Igf2. Mice carrying the *CRK10* mutation were crossed with Dis7CAS mice as described in the legend to Fig. 5. Dis7CAS mice are mostly *Mus domesticus* but are homozygous *M. castaneous* across the *H19*/*Igf2* locus (15). Allele-specific expression of *Igf2* was analyzed using the single-nucleotide primer extension (SNuPE) assay (36, 40).

RESULTS

A shared skeletal muscle enhancer for H19 and Igf2. In vivo transgenic analyses indicated that enhancers capable of driving transcription of *H19* in skeletal muscle lie between kb +13 and +36 (3, 10, 18, 20, 32). This region includes six short sequence elements that are well conserved between mice and humans and therefore are potentially important regulatory sites (18). In vitro transfection studies confirmed the presence of at least one set of skeletal muscle-specific enhancers in sequences centered between kb +22 and +28 (20). This 6-kb region includes one of the conserved sequence elements which had also been assayed by transient transgenesis and shown to drive expression of reporter constructs in midgestation embryos (18). To examine directly the requirement of these enhancer sequences for directing in vivo expression of *H19* and *Igf2* in skeletal muscle and in other mesodermal tissues, a 24-kb targeted deletion of sequences between kb 10.7 and 34.7 was constructed as shown in Fig. 1b. This *VM3* allele was constructed in two steps so that the selection marker encoding resistance to neomycin sulfate was removed prior to quantitation of *H19* and *Igf2* expression levels.

To determine whether the deleted elements are required for expression of *H19*, RNAs from pups inheriting the deletion via the maternal chromosome were analyzed by Northern blotting (Fig. 2a). Multiple samples from two mutant strains generated from independently derived cells lines were analyzed. *H19* levels in liver, heart, lung, gut, and kidney tissues were unaffected. In contrast, expression of *H19* in skeletal muscle and tongue tissue was reduced five- to sixfold compared with that of wild-type littermates. Thus, we concluded that the enhancer elements identified in transgene and transfection studies are, in fact, functional and necessary for expression of the *H19* gene in its normal chromosomal context. These enhancers are not required for all mesodermal expression but are specific to skeletal muscle.

To determine whether mesodermal expression of *H19* and *Igf2* is likely driven through a common set of enhancers, the effect of paternal-chromosome-based inheritance of the *VM3* deletion on *Igf2* expression was examined by Northern blotting (Fig. 2b). Qualitatively, the effects of the mutation were identical to those noted for *H19* on maternal-chromosome inheritance: *Igf2* RNA levels were normal in liver, heart, lung, gut, and kidney tissues, while expression in skeletal muscle and tongue tissue was reduced. Quantitatively, expression of *Igf2* in *VM3* mutants was 3.5 times lower than that in wild-type littermates. These results provided experimental evidence that *H19* and *Igf2* do have a common set of mesodermal enhancers. The location of these enhancers downstream of the *H19DMR* is consistent with the demands of the insulator model.

We did note some residual expression of *H19* and of *Igf2* in mutant mice. We noted this same level of expression even in pups that were homozygous for the *VM3* deletion allele (data not shown). Thus, we did not see any evidence for transvection at this locus. Rather, the residual expression is likely due to the activity of enhancer elements outside the *VM3* deletion. In situ hybridization experiments did not reveal any cell type-specific loss of expression in tongue tissue and skeletal muscle but rather showed a generalized decrease in transcript levels throughout these tissues (data not shown).

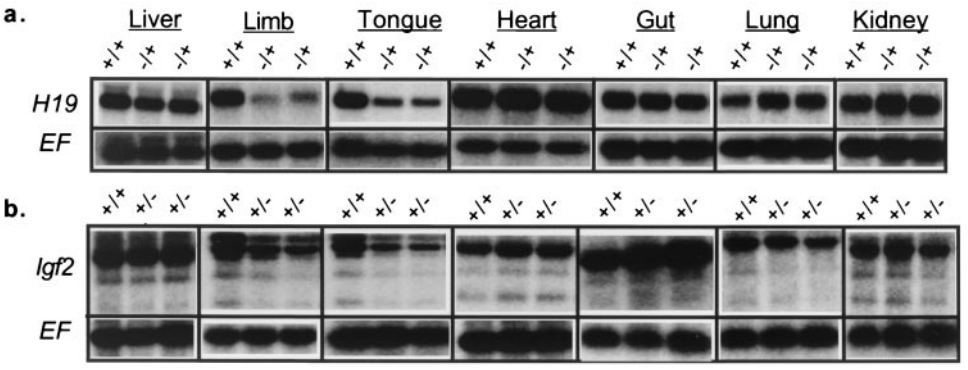

FIG. 2. Northern analysis demonstrating the effect of the *VM3* enhancer deletion on *H19* and *Igf2* expression. (a) *H19* RNA levels were examined in p2 pups inheriting the *VM3* mutation via the maternal chromosome (−/+). (b) *Igf2* RNA levels were examined in p2 pups inheriting the *VM3* mutation via the paternal chromosome (+/−). In both cases, mutants were compared to wild-type littermates (+/+). Blots were probed for *EF2a* to verify equal loading. For each tissue, RNA levels of at least two wild-type and two experimental animals from multiple independent litters were quantitated.

Nctc1 is not essential for normal mouse development. *Nctc1* is a skeletal-muscle-specific transcript that like *H19* is unlikely to encode a peptide product (19). The *VM3* mutation deletes the entire mRNA coding region for *Nctc1*. Since mice homozygous for the *VM3* mutation are viable as well as fertile and appear and behave normally, we concluded that *Nctc1* gene activity is not essential for normal mouse development. Although we consider it unlikely, we cannot rule out the possibility of a requirement for *Nctc1* transcription for activation of *H19* and *Igf2* in *cis*.

VM3 allele and L23mrp expression. The gene encoding the L23 (mitochondrion)-related protein (*L23mrp* or *Rpl23*), located 40 kb from the imprinted *H19* gene (Fig. 1a), is biallelically and ubiquitously expressed at low levels relative to embryonic *H19*. Targeted deletion of the endodermal enhancers located downstream of *H19* has no effect on *L23mrp* expression, suggesting that the latter gene is functionally insulated from *H19* (49). Likewise, we saw that mice homozygous for the *VM3* mesodermal enhancer deletion exhibited no loss of *L23mrp* expression in skeletal muscle, nor was there any increase in *L23mrp* transcription in fetal liver tissue (data not shown). Thus, the *VM3* deletion, which removes sequences to within 4 kb of the *L23mrp* transcriptional start site, has no effect on the mechanism insulating *L23mrp* from the *H19*/*Ig2* endodermal enhancers or on the mechanisms driving expression of *L23mrp* in muscle tissue.

VM3 and TNNT3 expression. The gene encoding the faster-migrating isoform of skeletal muscle troponin-T (*TNNT3*) is located 55 kb from *L23MRP* (47). The linkage of *Tnnt3* to *H19* is conserved in mice (27). *Tnnt3* is biallelically expressed and shows expression parallel to that of *H19* in different adult skeletal muscle types, which led to the suggestion that *H19* and *TNNT3* have common enhancer elements (47). However, mice homozygous for the *VM3* enhancer deletion exhibited no change in *Tnnt3* expression levels (data not shown).

Additional mesodermal enhancer sequences downstream of kb +35. Endoderm-specific enhancer elements shared by *H19* and *Igf2* were identified by deletion of sequences between kb +7.2 and +13 (26), while experiments described above demonstrated that some shared mesoderm-specific enhancer elements map to sequences centered at kb +26. Comparison of expression patterns of mice carrying YAC (3) and BAC (20) *H19* transgenes extending to about kb +36 and +140, respectively, suggested that additional enhancers capable of driving high levels of mesoderm-specific expression of *H19* in several tissues, including the gut, heart, lung, and kidney, are likely to lie downstream of kb +35. To test directly whether such enhancer elements play a role in expression of *H19* in its normal chromosomal context, we examined the effect of maternal-chromosome-based inheritance of the *CRK10* allele. The *CRK10* mutation is an insertion of a 9.2-kb element, including the *H19DMR*/*Igf2*-insulator, +10.7 kb downstream of the *H19* promoter (Fig. 1a).

As previously demonstrated, there was no loss of expression in the liver, consistent with the location of the endodermal enhancers upstream of the inserted insulator (Fig. 3a). As previously demonstrated for limb muscle, expression in the tongue was almost completely lost (Fig. 3a). This loss of expression in skeletal muscle is consistent with our above-described demonstration that transcription of *H19* in these tissues is dependent on enhancer elements downstream of the insulator insertion site as defined by the *VM3* deletion.

We next looked at tissues with significant contributions of cells of mesodermal origin but which were unaffected by the *VM3* deletion. Any effect unique to *CRK10* would presumably be due to the insulator-blocking enhancer elements that are downstream of kb +35. We noted a 50% reduction in *H19* RNA levels in the gut (Fig. 3a). By in situ hybridization, we determined that the loss of expression was specific to the smooth muscle layer, with continued high levels being noted in the epithelium (Fig. 3c). This is essentially reciprocal to the pattern seen on deletion of the endodermal enhancers (26). The pattern is also consistent with previous transgenic studies in which the endodermal enhancers were demonstrated to be capable of driving expression only in the endodermally derived endothelium (9).

We also noted a modest decrease in total mRNA levels in the heart (Fig. 3a). Since only about 50% of cardiac expression is blocked by the *CRK10* insulator insertion, and because expression in the heart is not altered by the *VM3* deletion or by

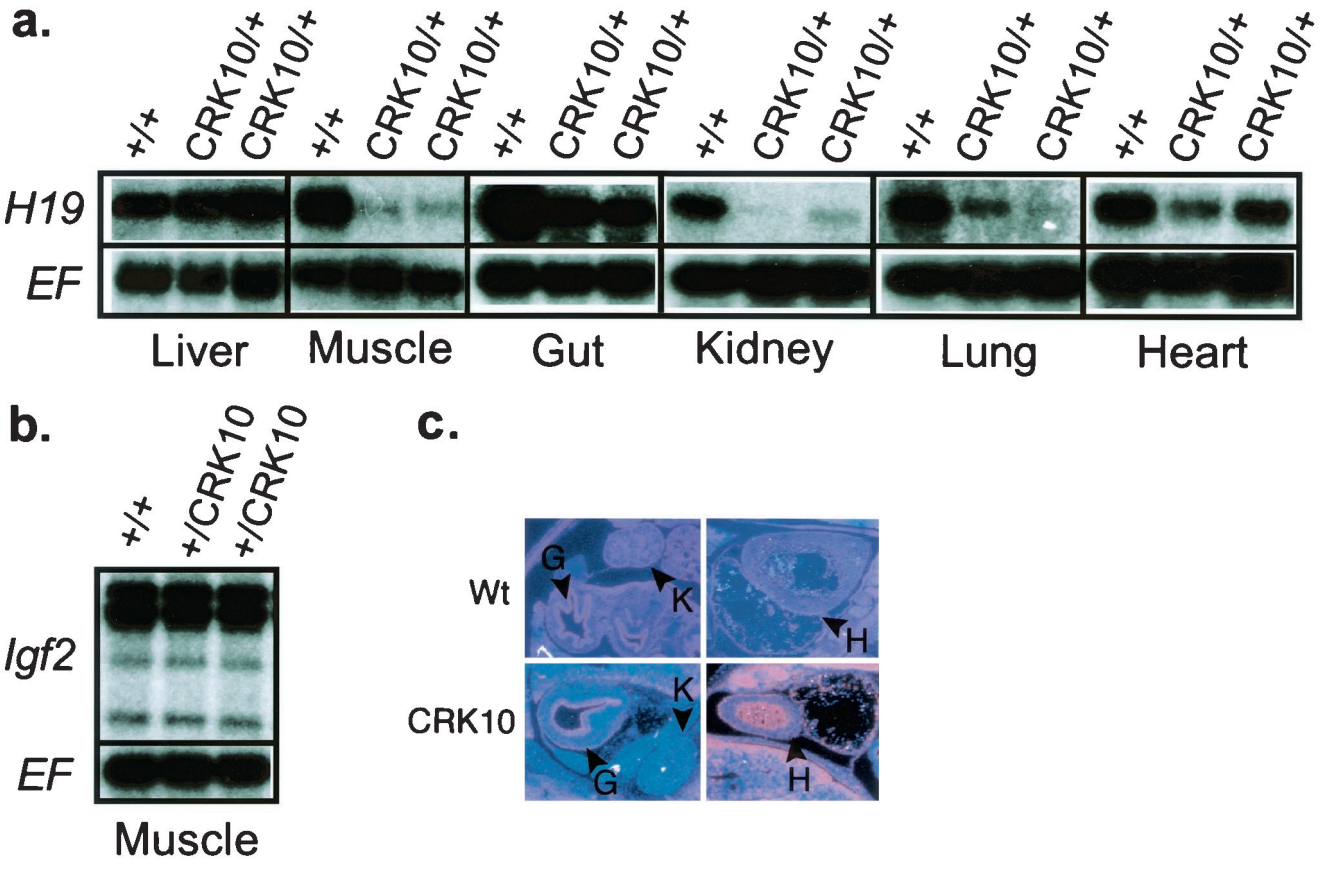

FIG. 3. Effect of the *CRK10* mutation on *H19* and *Igf2* expression. (a) *H19* RNA levels in embryonic day 18.5 pups inheriting the *CRK10* mutation via the maternal chromosome (*CRK10*/+) were analyzed by Northern blotting. (b) *Igf2* RNA levels in skeletal muscle of pups inheriting the mutation via the paternal chromosome (+/*CRK10*) were also examined by Northern blotting. Expression of wild type littermates (+/+) was also quantitated. Blots were probed with *EF2c* to verify equal loading. For each tissue, RNA levels of at least two wild-type and two experimental animals from multiple independent litters were quantitated. (c) In situ analysis of *H19* expression patterns in embryonic day 14 embryos. Wt, wild type; H, heart; G, gut; K, kidney.

the deletion of the enhancers centered at kb +8, the location of most cardiac enhancer activity remains puzzling.

The loss of *H19* expression from the *CRK10* chromosome in the lung and the kidney was almost complete (Fig. 3a). In contrast to the patterns seen in the heart and gut, the effect does not appear to be cell type specific; rather, the reduction in RNA levels appears to be uniform. Curiously, these results are very similar to what is seen on deletion of the endodermal enhancer (26).

Parent-of-origin-specific activity of the CRK10 insertion. Having demonstrated directly that *Igf2* shares the downstream mesoderm-specific enhancers necessary for expression in skeletal muscle, the effect of a paternal-chromosome-based inheritance of the *CRK10* insertion could be discerned by examining *Igf2* expression. The ability of the inserted insulator to block activation of *Igf2* by the distal skeletal muscle enhancers was studied. In contrast to its effect on *H19* upon maternal inheritance, the insulator did not have the ability to block transcription of the paternal *Igf2* allele (Fig. 3b). Rather, the paternal *Igf2* promoters continued to be expressed at high levels in skeletal muscle despite the presence in *cis* of the *CRK10* insertion separating them from the skeletal muscle enhancers. Thus, we concluded that the inserted insulator is not active on the paternal chromosome and therefore must be subject to the same parent-of-origin-specific modulation of its insulator function as is postulated in its normal location. These results are consistent with and perhaps were predicted by our previous finding that the ectopic insulator is specifically hypermethylated when inherited via the paternal chromosome (20).

Methylation activity of the CRK10 insertion. In its normal location, the *H19DMR* not only functions as a transcriptional insulator that blocks activation of the maternal *Igf2* promoter but also acts to direct methylation of cytosine residues in the paternal *H19* promoter. These epigenetic modifications are presumed to then be directly responsible for monoallelic repression of *H19*. To determine whether the inserted sequences act as a nucleation center for developmentally regulated modification of adjacent sequences, the methylation status of DNA located immediately downstream of the *CRK10* insertion was examined. Genomic DNAs were prepared from pups inheriting the *CRK10* insertion and from their wild-type littermates. These DNAs were subjected to restriction digestion with enzymes sensitive to methylation. Whether inherited via the maternal or paternal chromosome, endogenous sequences adja-

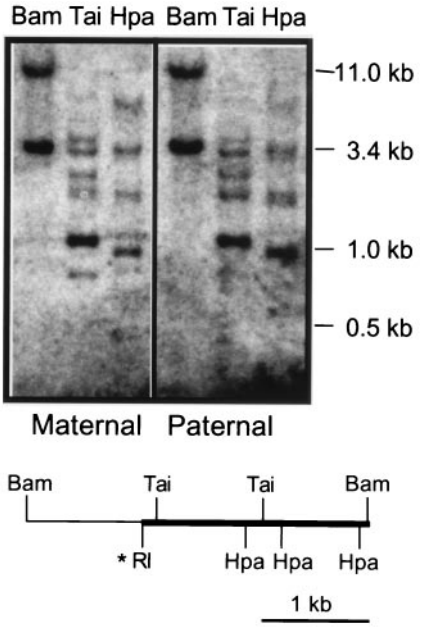

FIG. 4. Methylation analysis of sequences downstream of the *CRK10* insertion mutation. DNAs from heterozygous pups inheriting the *CRK10* mutation via the maternal or the paternal chromosome were digested with *Bam*HI and hybridized with an 2.4-kb *Eco*RI-*Bam*HI fragment from sequences immediately 3′ of the *CRK10* insertion. This hybridization reveals an 11-kb band specific to the wild-type chromosome and a 3.4-kb band specific to the *CRK10* chromosome. The 3.4-kb band is thus a junction fragment including 1 kb of sequences from the *H19DMR* (thin line on the diagram) and 2.4 kb of 3′-flanking sequences (thick line on the diagram). Topologically, these flanking sequences are in the same position relative to the inserted *H19DMR* as the endogenous *H19* promoter and gene body are to the endogenous *H19DMR*. To determine whether these flanking sequences are differentially methylated in a parent-of-origin-specific manner, aliquots of the *Bam*HI-digested DNA were also digested with methylation-sensitive enzymes, including *Tai*I (Tai) and *Hpa*II (Hpa). A restriction map of the 3.4-kb *Bam*HI fragment specific to the *CRK10* chromosome is depicted, with the probe shown as a thickened line. The thin line represents the sequences that are part of the *H19DMR* that was inserted at the *Eco*RI (RI) site.

cent to the inserted *H19DMR* remained unaffected; there was no apparent increase in CpG methylation of the downstream sequences (Fig. 4). Rather, the sequences in this region appear to be largely unmethylated.

Effect of insulator activity on Igf2 regulation. In light of recent data suggesting that insulators work in tandem to "loop out" genetic loci into regulatory domains (see Discussion), we next examined the effect of the *CRK10* mutation on maternal transcriptional regulation of *Igf2* in the liver and also in skeletal muscle. The relative contribution of the maternal *Igf2* allele was quantitated by SNuPE assay (24, 35). On the *CRK10* chromosome, the enhancer responsible for expression in the liver is flanked by insulator elements and is separated from the *Igf2* promoter by a single insulator, just as it is on the wild-type chromosome. As expected, we saw no expression of maternal *Igf2* from the *CRK10* chromosome in liver tissue (Fig. 5). However, we also did not detect any activation of maternal *Igf2* from the *CRK10* chromosome in skeletal muscle (Fig. 5), in which the relevant enhancer is separated from the promoter by

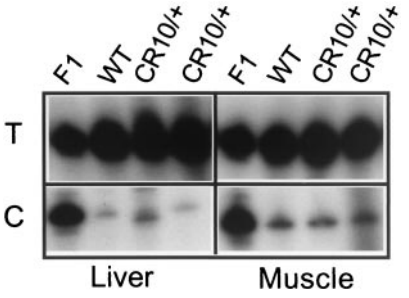

FIG. 5. Effect of maternal-chromosome-based inheritance of the *CRK10* mutation on *Igf2* expression. Skeletal muscle and liver RNA samples were treated with DNase I, amplified for *Igf2* by reverse transcription-PCR, and analyzed for allele-specific expression by SNuPE. Expression was analyzed in neonates inheriting the *CRK10* mutation with an *M. domesticus Igf2* allele via the maternal chromosome and inheriting a wild-type chromosome with an *M. castaneous Igf2* allele via the paternal chromosome (*CRK10*/+). Their control littermates likewise have maternal-chromosome-derived *domesticus* and paternal-chromosome-derived *M. castaneous* alleles of *Igf2*, but both chromosomes are wild type (+/+). Lane F1 is a control representing a 50:50 mix of *M. castaneous* and *M. domesticus* substrates. *M. domesticus* (or maternal) RNA results in incorporation of cytosine (C), and *M. casteneous* (or paternal) RNA results in incorporation of thymidine (T).

a paired set of functional insulators. Thus, as discussed below, pairing of insulators did not result in their inactivation in this mammalian system.

DISCUSSION

Transcriptional regulation of the *Igf2* and *H19* genes has been intensively studied because of the association of dysregulation at this locus with several human diseases and also as a primary model system for investigating mechanisms of genomic imprinting. The currently favored model for imprinting of the two genes posits that monoallelic expression of each gene depends on a common *cis*-acting element, the *ICE*, located just upstream of the *H19* promoter (Fig. 1) (34, 41). Sequences within this region are hypermethylated specifically on the paternal chromosome. This DNA methylation is postulated to enable expression of the *Igf2* gene by inactivating a transcriptional insulator. The paternal-chromosome-specific DNA methylation also induces developmentally programmed epigenetic changes at the *H19* promoter which silence it. This popular model requires that the enhancers for both *H19* and *Igf2* must be located downstream of the *H19* gene, while the coordinate expression patterns of the two genes suggest that these enhancers are likely to be shared.

Previous studies have demonstrated the corequirement of a common set of endodermal enhancer elements located downstream of *H19* (26). Here we examined a mouse with a targeted deletion of a region downstream of the *H19* gene which had previously been shown to have enhancer activity in vitro (20) and in transgenic lines (18, 20), and we directly demonstrated that the deleted sequences included the primary enhancer element important for skeletal muscle expression of both *H19* and *Igf2*. Northern analysis demonstrated that both the *H19* and *Igf2* RNA levels in the liver, heart, gut, lung, and kidney were unaffected by the deletion. In contrast, the *H19* and *Igf2*

RNA levels were reduced 5.5- and 3.5-fold, respectively, in skeletal muscle. The nonequivalent reduction in expression of the two genes suggests that expression of *Igf2* may also be driven by other mesodermal enhancers which are not utilized by *H19*. This hypothesis could explain recent reports demonstrating that monoallelic expression of *Igf2* requires sequences in addition to the *Igf2* insulator at the *ICE*/*H19DMR* (1, 12).

With verification that *H19* and *Igf2* both utilize skeletal muscle enhancers downstream of the insertion site at +10.7 kb, the parent-of-origin activity of the *CRK10* allele could be defined further. We first looked at paternal-chromosome inheritance and demonstrated that the *CRK10* insertion mutation has no effect on transcriptional regulation of *Igf2*. Just as in its normal location upstream of the *H19* gene, the insulator activity is parent-of-origin specific. Consistent with this finding, we had previously shown that the ectopic insulator remains unmethylated on the maternal chromosome but is specifically hypermethylated on paternal inheritance (20). Our results are in contrast with those obtained in a recent study by Hark and coworkers, in which the insulator activity of an ectopic *H19ICE* element was determined not to be parent-of-origin specific (17). In the latter study, the activity of a smaller insert encompassing only sequences between kb −3.8 and −0.8 was tested by using randomly integrated transgenic constructs. We are presently testing whether we were able to see maternal-chromosome-specific transcriptional insulation in our system because the genetic context of mouse distal chromosome 7 supplies crucial information or because of the additional sequences included in the *CRK10* insertion (i.e., sequences in addition to the *H19DMR*).

Further analysis of the *CRK10* allele revealed that the inserted *DMR* lacks the ability to affect the methylation status of adjacent sequences. Our experiments cannot distinguish between a requirement for particular target sequences, such as the relatively CpG-rich *H19* promoter, and a deficiency in the ectopic element's function.

Insertion of the *H19DMR* between the liver and skeletal-muscle enhancer elements located downstream of *H19* has confirmed the presence of downstream enhancer elements required for transcription of *H19* in the mesoderm. Interestingly, the *CRK10* mutation almost completely abolished *H19* expression in the lung and kidney. Previous transgenic and deletion analyses have shown that endodermal enhancers required for both genes are located around kb 8 (10, 26). Deletion of this region caused a complete loss of *H19* expression in the lung and kidney. Similarly, the insertion of an insulator at kb +10 caused an almost complete loss of *H19* expression in those tissues. Together these results suggest that there are at least two required sets of enhancer elements necessary for the transcription of *H19* in these tissues. Although these enhancers are very distant on the chromosome, their effects are extremely synergistic. This model explains the puzzling inability of the proximal endodermal enhancers to direct high levels of expression in kidney and lung tissues in transgenic mice (10, 32, 45) even while their necessity in these same tissues was demonstrated through deletion mutations. Future studies will examine the nature of the synergism to determine whether this is a mechanism for specifically directing the enhancers to *H19* and *Igf2* to the exclusion of other genes within striking distance of the enhancers.

Insulators are thought to play an important role in gene regulation. At least two models for insulator action have been proposed. In one case, the insulator is predicted to block the progress of a positive signal that moves from the enhancer toward the promoter. In a second model, insulators regulate gene activity by organizing loci into transcriptionally active and transcriptionally inactive domains (5, 37). Very recent studies examining the effect of paired insulator elements in *Drosophila* support the notion that insulators regulate enhancer-promoter interactions through the formation of chromatin loops (11, 28). In these experiments, an enhancer flanked by the *Su*(*Hw*) insulator was unable to interact with its promoter. However, when an enhancer was separated from its promoter by a paired set of insulators, the enhancer retained the ability to activate that promoter. It was proposed that two insulators work in tandem to loop out any intervening DNA between them and leave the enhancer and promoter elements, which remain in a single active domain, thus allowing the enhancer-promoter interactions. (See also a review by Bell et al. [6].)

To examine this model in a mammalian system, we returned to the *CRK10* chromosome, whose organization relative to the *Igf2* promoter mirrors that of the transgenic constructs used in the *Drosophila* experiments (Fig. 1a). The analysis was designed not to determine the minimal sequences required for insulator function but rather to determine a possible role for functional insulators in organizing the locus into independent arrays. On a maternal *CRK10* chromosome, the endodermal enhancer sequences that drive expression of *Igf2* and *H19* in the liver are flanked by two functional insulator elements, but only a single insulator lies between the enhancer sequences and the *Igf2* promoter. However, the skeletal-muscle-specific enhancer is separated from the *Igf2* promoter by paired insulator elements. We examined expression of *Igf2* specifically from the maternal *CRK10* chromosome because we already knew from examination of *H19* expression that the enhancers and the insulators were all functioning. In contrast to results demonstrated in *Drosophila* for the *Su*(*Hw*) insulator, the maternal *Igf2* promoter remained silent not only in the liver but also in skeletal muscle. Thus, in the mammalian *Igf2*-insulator system, we do not see evidence for looping; instead, the very large distances over which the insulators and enhancers work in this system may be more supportive of alternate models for insulator function (5, 13).

REFERENCES

1. **Ainscough, J. F., R. John, S. Barton, and M. Surani.** 2000. A skeletal muscle-specific mouse *Igf2* repressor lies 40 kb downstream of the gene. Development **127:**3923–3930.
2. **Ainscough, J. F., L. Dandola, and M. A. Surani.** 2000. Appropriate expression of the mouse *H19* gene utilises three or more distinct enhancer regions spread over more than 130 kb. Mech. Dev. **91:**365–368.
3. **Ainscough, J. F., T. Koide, M. Tada, S. Barton, and M. A. Surani.** 1997. Imprinting of *Igf2* and *H19* from a 130 kb YAC transgene. Development **124:**3621–3632.
4. **Bartolomei, M. S., A. L. Webber, M. E. Brunkow, and S. M. Tilghman.** 1993. Epigenetic mechanisms underlying the imprinting of the mouse *H19* gene. Genes Dev. **7:**1663–1673.
5. **Bell, A., and G. Felsenfeld.** 1999. Stopped at the border: boundaries and insulators. Curr. Opin. Genet. Dev. **9:**191–198.
6. **Bell, A., A. West, and G. Felsenfeld.** 2001. Insulators and boundaries: versatile regulatory elements in the eukaryotic genome. Science **291:**447–450.
7. **Bell, A. C., and G. Felsenfeld.** 2000. Methylation of a CTCF-dependent boundary controls imprinted expression of the *Igf2* gene. Nature **405:**482–485.
8. **Brandeis, M., T. Kafri, M. Ariel, J. R. Chaillet, J. McCarrey, A. Razin, and H. Cedar.** 1993. The ontogeny of allele-specific methylation associated with

imprinted genes in the mouse. EMBO J. **12:**3669–3677.
9. **Brenton, J. D., R. A. Drewell, S. Viville, K. J. Hilton, S. C. Barton, J. F. Ainscough, and M. A. Surani.** 1999. A silencer element identified in *Drosophila* is required for imprinting of *H19* reporter transgenes in mice. Proc. Natl. Acad. Sci. USA **96:**9242–9247.
10. **Brunkow, M. E., and S. M. Tilghman.** 1991. Ectopic expression of the *H19* gene in mice causes prenatal lethality. Genes Dev. **5:**1092–1101.
11. **Cai, H., and P. Shen.** 2001. Effects of *cis* arrangements of chromatin insulators on enhancer-blocking activity. Science **291:**493–495.
12. **Constancia, M., W. Dean, S. Lopes, T. Moore, G. Kelsey, and W. Reik.** 2000. Deletion of a silencer element in *Igf2* results in loss of imprinting independent of *H19*. Nat. Genet. **26:**203–206.
13. **Dorsett, D.** 1999. Distant liaisons: long-range enhancer-promoter interactions in *Drosophila*. Curr. Opin. Genet. Dev. **9:**505–514.
14. **Ferguson-Smith, A. C., H. Sasaki, B. M. Cattanach, and M. A. Surani.** 1993. Parental-origin-specific epigenetic modifications of the mouse *H19* gene. Nature **362:**751–755.
15. **Gould, T. D., and K. Pfeifer.** 1998. Imprinting of mouse *Kvlqt1* is developmentally regulated. Hum. Mol. Genet. **7:**483–487.
16. **Hark, A. T., and S. M. Tilghman.** 1998. Chromatin conformation of the *H19* epigenetic mark. Hum. Mol. Genet. **7:**1979–1985.
17. **Hark, A. T., C. J. Schoenherr, D. J. Katz, R. S. Ingram, J. M. Levorse, and S. M. Tilghman.** 2000. CTCF mediates methylation-sensitive enhancer blocking activity at the *H19*/*Igf2* locus. Nature **405:**486–489.
18. **Ishihara, K., N. Hatano, H. Furuumi, R. Kato, T. Iwaki, K. Miura, Y. Jinno, and H. Sasaki.** 2000. Comparative genomic sequencing identifies novel tissue-specific enhancers and sequence elements for methylation-sensitive factors implicated in *Igf2*/*H19* imprinting. Genome Res. **10:**664–671.
19. **Ishihara, K., R. Kato, H. Furuumi, M. Zubair, and H. Sasaki.** 1998. Sequence of a 42-kb mouse region containing the imprinted *H19* locus: identification of a novel muscle-specific transcription unit showing biallelic expression. Mamm. Genome **9:**775–777.
20. **Kaffer, C. R., M. Srivastava, K. Park, E. Ives, S. Hsieh, J. Batlle, A. Grinberg, S. P. Huang, and K. Pfeifer.** 2000. A transcriptional insulator at the imprinted *H19*/*Igf2* Locus. Genes Dev. **14:**1908–1919.
21. **Kanduri, C., C. Holmgren, M. Pilartz, G. Franklin, M. Kanduri, L. Liu, V. Ginjala, E. Ulleras, R. Mattsson, and R. Ohlsson.** 2000. The 5′-flanking of the murine *H19* gene in unusual chromatin conformation unidirectionally blocks enhancer-promoter communication. Curr. Biol. **10:**449–457.
22. **Kanduri, C., V. Pant, D. Loukinov, E. Pugacheva, C. Qi, A. Wolffe, R. Ohlsson, and V. Lobanenkov.** 2000. Functional association of CTCF with the insulator upstream of the *H19* gene is parent-of-origin specific and methylation-sensitive. Curr. Biol. **10:**853–856.
23. **Khosla, S., A. Aitchison, R. Gregory, N. D. Allen, and R. Feil.** 1999. Parental allele-specific chromatin configuration in a boundary–imprinting-control element upstream of the mouse *H19* gene. Mol. Cell. Biol. **19:**2556–2566.
24. **Kuppuswamy, M. N., J. W. Hoffmann, C. K. Kasper, S. G. Spitzer, S. L. Groce, and S. P. Bajaj.** 1991. Single nucleotide primer extension to detect genetic diseases: experimental application to hemophilia B (factor IX) and cystic fibrosis. Proc. Natl. Acad. Sci. USA **88:**1143–1147.
25. **Lasko, M., J. Picher, J. Gorman, B. Sauer, Y. Okamoto, E. Lee, F. Alt, and H. Westphal.** 1996. Efficient in vivo manipulation of mouse genomic sequences at the zygote stage. Proc. Natl. Acad. Sci. USA **93:**5860–5865.
26. **Leighton, P. A., J. R. Saam, R. S. Ingram, C. L. Stewart, and S. M. Tilghman.** 1995. An enhancer deletion affects both *H19* and *Igf2* expression. Genes Dev. **9:**2079–2089.
27. **Misener, V., A. Wielowieyski, L. Brennan, G. Beebakhee, and J. Jongstra.** 1998. The mouse *Lsp1* and *Tnnt3* genes are 4.3 kb apart on distal mouse chromosome 7. Mamm. Genome **9:**846–848.
28. **Muravyova, E., A. Golovnin, E. Gracheva, A. Parshikov, T. Belenkaya, V. Pirrotta, and P. Georgiev.** 2001. Loss of insulator activity by paired *Su*(*Hw*) chromatin insulators. Science **291:**495–498.
29. **Olek, A., J. Walter, B. Horsthemke, B. Dittrich, and K. Buiting.** 1997. The pre-implantation ontogeny of the H19 methylation imprint. Nat. Genet. **17:**275–276.
30. **Onyango, P., W. Miller, J. Lehoczky, C. Leung, B. Birren, S. Wheelan, K. Dewar, and A. Feinberg.** 2000. Sequence and comparative analysis of the mouse 1-megabase region orthologous to the human 11p15.5 imprinted domain. Genome Res. **10:**1697–1710.
31. **Paulsen, M., K. R. Davies, L. M. Bowden, A. J. Villar, O. Franck, M. Fuermann, W. L. Dean, K. R. Moore, N. Rodrigues, K. E. Davies, R.-J. Hu, A. P. Feinberg, E. R. Maher, W. Reik, and J. Walter.** 1998. Syntenic organization of the mouse distal chromosome 7 imprinting cluster and the Beckwith-Wiedemann syndrome region in chromosome 11p15.5 Hum. Mol. Genet. **7:**1149–1159.
32. **Pfeifer, K., P. A. Leighton, and S. M. Tilghman.** 1996. The structural *H19* gene is required for transgene imprinting. Proc. Natl. Acad. Sci. USA **93:** 13876–13883.
33. **Reik, W., M. Constancia, W. Dean, K. Davies, L. Bowden, A. Murrell, R. Feil, J. Walter, and G. Kelsey.** 2000. *Igf2* imprinting in development and disease. Int. J. Dev. Biol. **44:**145–150.
34. **Reik, W., and A. Murrell.** 2000. Genomic imprinting. Silence across the border. Nature **405:**408–409.
35. **Singer-Sam, J., V. Chapman, J. M. LeBon, and A. D. Riggs.** 1992. Parental imprinting studies by allele-specific primer extension after PCR: paternal X chromosome-linked genes are transcribed prior to preferential paternal X chromosome inactivation. Proc. Natl. Acad. Sci. USA **89:**10469–10473.
36. **Srivastava, M., S. Hsieh, A. Grinberg, L. Williams-Simon, S.-P. Huang, and K. Pfeifer.** 2000. *H19* and *Igf2* monoallelic expression is regulated in two distinct ways by a shared *cis* acting element. Genes Dev. **14:**1186–1195.
37. **Sun, F., and S. Elgin.** 1999. Putting boundaries on silence. Cell **99:**459–462.
38. **Szabo, P., S. Tang, A. Rentsendorj, G. Pfeifer, and J. R. Mann.** 2000. Maternal-specific footprints at putative CTCF sites in the *H19* imprinting control region give evidence for insulator function. Curr. Biol. **10:**607–610.
39. **Szabo, P. E., G. P. Pfeifer, and J. R. Mann.** 1998. Characterization of novel parent-specific epigenetic modifications upstream of the imprinted mouse *H19* gene. Mol. Cell. Biol. **18:**6767–6776.
40. **Szabo, P. E., and J. R. Mann.** 1995. Biallelic expression of imprinted genes in the mouse germ line: implications for erasure, establishment, and mechanisms of genomic imprinting. Genes Dev. **9:**1857–1868.
41. **Thorvaldsen, J., and M. S. Bartolomei.** 2000. Mothers setting boundaries. Science **288:**2145–2146.
42. **Thorvaldsen, J. L., K. L. Duran, and M. S. Bartolomei.** 1998. Deletion of the *H19* differentially methylated domain results in loss of imprinted expression of *H19* and *Igf2*. Genes Dev. **12:**3693–3702.
43. **Tremblay, K. D., K. L. Duran, and M. S. Bartolomei.** 1997. A 5′ 2-kilobase-pair region of the imprinted mouse *H19* gene exhibits exclusive paternal methylation throughout development. Mol. Cell. Biol. **17:**4322–4329.
44. **Tremblay, K. D., J. R. Saam, R. S. Ingram, S. M. Tilghman, and M. S. Bartolomei.** 1995. A paternal-specific methylation imprint marks the alleles of the mouse *H19* gene. Nat. Genet. **9:**407–413.
45. **Webber, A., R. I. Ingram, J. Levorse, and S. M. Tilghman.** 1998. Location of enhancers is essential for imprinting of *H19* and *Igf2*. Nature **391:**711–715.
46. **Yoo-Warren, H., V. Pachnis, R. S. Ingram, and S. M. Tilghman.** 1988. Two regulatory domains flank the mouse H19 gene. Mol. Cell. Biol. **8:**4707–4715.
47. **Yuan, L., N. Qian, and B. Tycko.** 1996. An extended region of biallelic gene expression and rodent-human synteny downstream of the imprinted *H19* gene on chromosome 11p15.5. Hum. Mol. Genet. **5:**1931–1937.
48. **Zemel, S., M. S. Bartolomei, and S. M. Tilghman.** 1992. Physical linkage of two mammalian imprinted genes. Nat. Genet. **2:**61–65.
49. **Zubair, M., K. Hilton, J. Saam, M. Surani, S. Tilghman, and H. Sasaki.** 1997. Structure and expression of the mouse *L23mrp* gene downstream of the imprinted *H19* gene: biallelic expression and lack of interaction with *H19* enhancers. Genomics **45:**290–296.